

Atmospheric Chemistry of Diethyl Methylphosphonate, Diethyl Ethylphosphonate, and Triethyl Phosphate

Sara M. Aschmann, Ernesto C. Tuazon, and Roger Atkinson^{*,†}

Air Pollution Research Center, University of California, Riverside, California 92521

Received: November 20, 2004; In Final Form: January 18, 2005

Rate constants for the reactions of OH radicals and NO₃ radicals with diethyl methylphosphonate [DEMP, (C₂H₅O)₂P(O)CH₃], diethyl ethylphosphonate [DEEP, (C₂H₅O)₂P(O)C₂H₅], and triethyl phosphate [TEP, (C₂H₅O)₃PO] have been measured at 296 ± 2 K and atmospheric pressure of air using relative rate methods. The rate constants obtained for the OH radical reactions (in units of 10⁻¹¹ cm³ molecule⁻¹ s⁻¹) were as follows: DEMP, 5.78 ± 0.24; DEEP, 6.45 ± 0.27; and TEP, 5.44 ± 0.20. The rate constants obtained for the NO₃ radical reactions (in units of 10⁻¹⁶ cm³ molecule⁻¹ s⁻¹) were the following: DEMP, 3.7 ± 1.1; DEEP, 3.4 ± 1.4; and TEP, 2.4 ± 1.4. For the reactions of O₃ with DEMP, DEEP, and TEP, an upper limit to the rate constant of <6 × 10⁻²⁰ cm³ molecule⁻¹ s⁻¹ was determined for each compound. Products of the reactions of OH radicals with DEMP, DEEP, and TEP were investigated using in situ atmospheric pressure ionization mass spectrometry (API-MS) and, for the TEP reaction, gas chromatography with flame ionization detection (GC-FID) and in situ Fourier transform infrared (FT-IR) spectroscopy. The API-MS analyses show that the reactions are analogous, with formation of one major product from each reaction: C₂H₅OP(O)(OH)CH₃ from DEMP, C₂H₅OP(O)(OH)C₂H₅ from DEEP, and (C₂H₅O)₂P(O)OH from TEP. The FT-IR and GC-FID analyses showed that the major products (and their molar yields) from the TEP reaction are (C₂H₅O)₂P(O)OH (65–82%, initial), CO₂ (80 ± 10%), and HCHO (55 ± 5%), together with lesser yields of CH₃CHO (11 ± 2%), CO (11 ± 3%), CH₃C(O)OONO₂ (8%), organic nitrates (7%), and acetates (4%). The probable reaction mechanisms are discussed.

Introduction

Volatile organic compounds emitted into the troposphere can undergo photolysis (at wavelengths >290 nm), react with OH radicals, react with NO₃ radicals, and react with O₃.¹ Alkyl and aryl phosphates [(RO)₃PO] and alkyl phosphonates [(RO)₂P(O)R], where R = aryl or alkyl, are used as plasticizers, flame retardants and fire-resistant fluids and lubricants, and organophosphorus compounds of structure (RO)₃PO and (RO)₃PS are widely used as pesticides.^{2,3} These compounds and their precursors may be released into the atmosphere where they can undergo transport and chemical transformations. While the kinetics of the atmospheric reactions of a number of simple “model” alkyl phosphates, alkyl phosphorothioates, and alkyl phosphonates of structure (RO)_nP(O)(SR)_{3-n}, (RO)_nP(S)(SR)_{3-n}, and (RO)₂P(O)X (R = CH₃ or C₂H₅ and X = H or CH₃) have been studied,^{4–8} the only compounds with R ≠ CH₃ for which data have been reported are triethyl phosphate [TEP, (C₂H₅O)₃PO] and diethyl methylphosphonate [DEMP, (C₂H₅O)₂P(O)CH₃].^{6,7} For the alkyl phosphates and alkyl phosphorothioates studied to date, reaction with the OH radical is the dominant atmospheric loss process,^{4,5} and only upper limits to the rate constants have been reported for the NO₃ radical and O₃ reactions.^{4,5}

To further investigate the reactivity of the alkyl groups attached directly to the phosphorus atom in alkyl phosphonates (i.e., of X in (RO)₂P(O)X), we have measured rate constants

for the gas-phase reactions of OH radicals, NO₃ radicals, and O₃ with diethyl methylphosphonate [DEMP, (C₂H₅O)₂P(O)CH₃], diethyl ethylphosphonate [DEEP, (C₂H₅O)₂P(O)C₂H₅], and triethyl phosphate [TEP, (C₂H₅O)₃PO], and we investigated the products of the atmospherically dominant OH radical reactions.

Experimental Methods

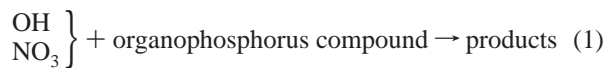
Most experiments were carried out at 296 ± 2 K and 740 Torr total pressure of purified air at ~5% relative humidity in two ~7000 L volume Teflon chambers, each equipped with two parallel banks of blacklamps for irradiation and a Teflon-coated fan to ensure rapid mixing of reactants during their introduction into the chamber. One of the Teflon chambers was interfaced to a PE SCIEX API III MS/MS direct air sampling, atmospheric pressure ionization tandem mass spectrometer (API-MS). Experiments utilizing in situ Fourier transform infrared (FT-IR) spectroscopy were carried out at 298 ± 2 K and 740 Torr total pressure of synthetic air (80% N₂ + 20% O₂) in a 5870 L Teflon-coated, evacuable chamber equipped with a multiple reflection optical system interfaced to a Mattson Galaxy 5020 FT-IR spectrometer.⁸ Irradiation was provided by a 24 kW xenon arc lamp, with the light being filtered through a 6 mm thick Pyrex pane to remove wavelengths <300 nm. IR spectra were recorded with 32 scans per spectrum (corresponding to a 1.2 min averaging time) at a full width at half-maximum resolution of 0.7 cm⁻¹ and a path length of 62.9 m.

Kinetic Studies. Rate constants for the reactions of OH and NO₃ radicals with DEMP, DEEP, and TEP were measured using relative rate techniques in which the concentrations of the organophosphorus compound and a reference compound (whose

[†] Also Department of Environmental Sciences and Department of Chemistry.

* To whom correspondence should be addressed: e-mail ratkins@mail.ucr.edu; Tel (951) 827-4191.

OH radical or NO₃ radical reaction rate constant is reliably known) were measured in the presence of OH or NO₃ radicals.^{5,9}



Providing that the organophosphorus compound and the reference compound reacted only with OH radicals or NO₃ radicals, then

$$\ln \left(\frac{[\text{organophosphorus}]_{t_0}}{[\text{organophosphorus}]_t} \right) - D_t = \frac{k_1}{k_2} \ln \left(\frac{[\text{reference compound}]_{t_0}}{[\text{reference compound}]_t} \right) - D_t \quad (I)$$

where [organophosphorus]_{t₀} and [reference compound]_{t₀} are the concentrations of the organophosphorus compound and reference compound, respectively, at time t₀, [organophosphorus]_t and [reference compound]_t are the corresponding concentrations at time t, D_t is a factor to account for dilution caused by any additions to the chamber during the experiments (D_t = 0 for the OH radical reactions and D_t = 0.0014 per N₂O₅ addition to the chamber in the NO₃ radical reactions), and k₁ and k₂ are the rate constants for reactions 1 and 2, respectively.

Hydroxyl radicals were generated in the presence of NO by the photolysis of methyl nitrite in air at wavelengths >300 nm.^{5,9} The initial reactant concentrations (molecules cm⁻³) employed for the OH radical reactions were CH₃ONO, ~2.4 × 10¹⁴; NO, ~2.4 × 10¹⁴; and organophosphorus compound(s) and reference compound(s), ~2.4 × 10¹³ each. The reference compounds used were α-pinene, 1,3,5-trimethylbenzene, and, in selected experiments as a check on the system, di-n-butyl ether, and irradiations were carried out at 20% of the maximum light intensity for 2.5–13 min. Experiments were also conducted to investigate the importance of dark decay and photolysis of ~2.4 × 10¹³ molecules cm⁻³ of DEMP, DEEP, and TEP in the chamber, with 8.0 × 10¹⁵ molecules cm⁻³ of cyclohexane also being present in the photolysis experiments to scavenge any OH radicals formed. While most experiments were carried out in air (21% O₂ content) at ~5% relative humidity, experiments were also carried out at 6%, 77%, and 78% O₂ content (with a relative humidity of <5%) and in air at 47% and 50% relative humidity.

Nitrate radicals were produced from the thermal decomposition of N₂O₅,¹⁰ and NO₂ was also included in the reactant mixtures. The initial reactant concentrations (molecules cm⁻³) were DEMP, DEEP, or TEP and methacrolein, propene, or 1-butene (the reference compounds), ~2.4 × 10¹³ each; NO₂, (4.8–9.6) × 10¹³, and two additions of N₂O₅ (each addition corresponding to (1.1–1.2) × 10¹⁴ molecules cm⁻³ of N₂O₅ in the chamber) were made to the chamber during an experiment.

The concentrations of the organophosphorus compounds and the reference compounds were measured during the experiments by gas chromatography with flame ionization detection (GC-FID). For the analyses of propene and 1-butene, gas samples were collected from the chamber into 100 cm³ volume all-glass gastight syringes and transferred via a 1 cm³ gas sampling loop onto a 30 m DB-5 megabore column initially held at -25 °C and then temperature-programmed to 200 °C at 8 °C min⁻¹. For the analyses of methacrolein, α-pinene, 1,3,5-trimethylbenzene, di-n-butyl ether, DEEP, DEMP, TEP, and, in product

studies (see below), acetaldehyde, 100 cm³ volume gas samples were collected from the chamber onto Tenax-TA solid adsorbent, with subsequent thermal desorption at ~250 °C onto a 30 m DB-1701 megabore column held at -40 or 0 °C and then temperature-programmed to 200 °C at 8 °C min⁻¹. Based on replicate analyses in the chamber in the dark, the analytical uncertainties for the organophosphorus compounds and the reference compounds used were typically ≤3%.

The rate constants, or upper limits thereof, for the reactions of DEMP, DEEP, and TEP with O₃ were determined by monitoring the decay of the organophosphorus compound in the presence of a known concentration of O₃,⁹ with cyclohexane being present to scavenge any OH radicals formed. Assuming that under these conditions the only loss process for DEMP, DEEP or TEP is by reaction with O₃, then

$$\ln([\text{organophosphorus}]_{t_0}/[\text{organophosphorus}]_t) - D_t = k_3[\text{O}_3](t - t_0) \quad (II)$$

where [organophosphorus]_{t₀} and [organophosphorus]_t are the concentrations of DEMP, DEEP, or TEP at times t₀ and t, respectively, D_t (= 0.0025) is the small amount of dilution caused by the initial addition of O₃ to the chamber, and k₃ is the rate constant for reaction 3.



The initial reactant concentrations (molecules cm⁻³) were DEMP, DEEP, or TEP, ~2.4 × 10¹³; O₃, (4.64–5.17) × 10¹³; and cyclohexane, (0.80–1.60) × 10¹⁶. O₃ concentrations were measured during the ~5.0 h duration reactions by ultraviolet absorption using a Dasibi model 1003-AH ozone analyzer, and the concentrations of DEMP, DEEP, and TEP were measured by GC-FID as described above.

Products of the OH Radical Reactions. Products of the reactions of OH radicals with DEMP, DEEP, and TEP were investigated using in situ API-MS analyses. In addition, products of the TEP reaction were investigated using in situ FT-IR spectroscopy and GC-FID. Experiments with GC-FID analyses for TEP and CH₃CHO were carried out in a ~7000 L Teflon chamber as described above for the kinetic experiments, except that the reference compound was not present.

Experiments with API-MS Analyses. In these experiments, the chamber contents were sampled through a 25 mm diameter × 75 cm length Pyrex tube at ~20 L min⁻¹ directly into the API mass spectrometer source. The operation of the API-MS in the MS (scanning) and MS/MS [with collision activated dissociation (CAD)] modes has been described previously.^{11,12} Use of the MS/MS mode with CAD allows the “product ion” or “precursor ion” spectrum of a given ion peak observed in the MS scanning mode to be obtained.¹¹ Both positive and negative ion modes were used in this work, with the majority of the data obtained being in the negative ion mode. In the positive ion mode, protonated water hydrates (H₃O⁺(H₂O)_n) generated by the corona discharge in the chamber diluent air were responsible for the protonation of analytes. Ions are drawn by an electric potential from the ion source through the sampling orifice into the mass-analyzing first quadrupole or third quadrupole. Neutral molecules and particles are prevented from entering the orifice by a flow of high-purity nitrogen (“curtain gas”), and as a result of the declustering action of the curtain gas on the hydrated ions, the ions that are mass analyzed are mainly protonated molecular ions ([M + H]⁺) and their protonated homo- and heterodimers.¹¹

In the negative ion mode, negative ions are generated by the negative corona around the discharge needle. The superoxide ion (O_2^-), its hydrates, and O_2 clusters are the major negative ions in the chamber diluent air. Other reagent ions, for example, NO_2^- and NO_3^- , are then formed from reactions between the primary reagent ions and neutral molecules such as NO_2 , and instrument tuning and operation were designed to induce cluster formation.¹² The initial concentrations of CH_3ONO and NO , and of DEMP, DEEP, or TEP, were $\sim 2.4 \times 10^{13}$ molecules cm^{-3} each, and irradiations were carried out for up to 2 min, resulting in up to $\sim 45\%$ reaction of the initially present DEMP, DEEP, or TEP.

Experiments with FT-IR Analyses. Irradiations of CH_3ONO [or $(\text{CH}_3)_2\text{CHONO}$]- NO -TEP mixtures in dry and humidified (5% relative humidity) air were carried out in the evacuable chamber, and both FT-IR and GC-FID analyses were employed. To investigate the formation of HCHO , the photolysis of 2-propyl nitrite^{8,13} was used as the OH radical source (photolysis of methyl nitrite forms HCHO , while photolysis of 2-propyl nitrite leads to acetone formation^{8,13}). To coordinate FT-IR and GC analyses, the irradiations were carried out intermittently, each with 3–8 min duration, for up to a total irradiation time of 16 min, with GC-FID analyses during the intervening dark periods and FT-IR spectra of the reaction mixture being recorded before and after each irradiation period. The initial concentrations (in units of 10^{13} molecules cm^{-3}) employed were TEP, 2.4–6.4; CH_3ONO , 24.6, or $(\text{CH}_3)_2\text{CHONO}$, 19.7; and NO , 24.6. A weighed amount of liquid TEP in a sample tube was introduced into the chamber by heating and flushing with a stream of heated N_2 gas. Partial pressures of CH_3ONO (or $(\text{CH}_3)_2\text{CHONO}$) and NO in calibrated 2 L Pyrex bulbs were measured in a vacuum manifold with a 100 Torr MKS Baratron and flushed into the chamber with N_2 .

Vapor spectra of $(\text{C}_2\text{H}_5\text{O})_2\text{P}(\text{O})\text{OH}$ (diethyl phosphate, DEP) were obtained by heating the liquid sample and flushing into the chamber with a stream of heated N_2 gas. However, the calibration for these spectra could not be determined directly from the known amount injected due to the rapid loss of the compound to the chamber walls. Attempts at calibration with the use of a heated, 15 cm path length Pyrex cell with NaCl windows attached by epoxy resin failed. Therefore, an estimate of the gas-phase absorption coefficient of the strongest IR band of DEP was obtained from measurements of the IR spectra of DEP in CH_2Cl_2 solution using a sealed 1.09 mm path length NaCl liquid cell. Molar concentrations of DEP in the range 0.001–0.005 were used, resulting in an average integrated absorption coefficient (baseline corrected) for the absorption band(s) in the 922–1128 cm^{-1} region of 8.2×10^{-17} cm molecule^{-1} (base 10). Measurements using solutions in cyclopentane, a nonpolar solvent, were in excellent agreement with those from CH_2Cl_2 solutions for comparable segments of the band envelope. The above absorption coefficient was then used to estimate the concentrations which corresponded to the spectra recorded for a sample of DEP introduced as vapor into the evacuable chamber as described above. One of these quantified gas-phase DEP spectra was then employed for analysis of DEP in irradiated CH_3ONO - NO -TEP-air mixtures. The use of this indirect calibration of the DEP IR absorption coefficient has a probable error of $\sim \pm 20\%$. Figure 1 illustrates the absorption band contours of DEP in the vapor state and in dichloromethane and cyclopentane solutions.

Chemicals. The chemicals used, and their stated purities, were diethyl ethylphosphonate (98%), Lancaster; acetaldehyde (99.5+%), diethyl methylphosphonate (97%), di-*n*-butyl ether

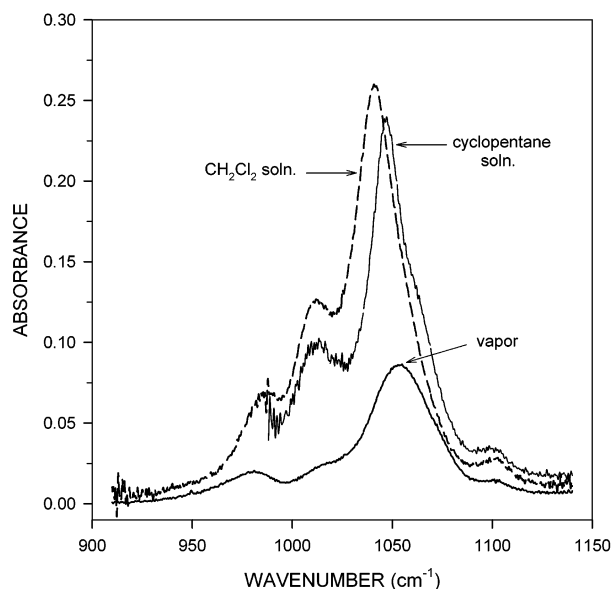


Figure 1. Band envelopes of diethyl phosphate (DEP) in dichloromethane solution (2.36×10^{-3} mol L^{-1} , 1.09 mm path length cell), cyclopentane solution (2.20×10^{-3} mol L^{-1} , 1.09 mm path length cell), and vapor phase (calculated to be 8.4×10^{12} molecules cm^{-3} , 62.9 m path). Cyclopentane has a narrower transmission window in this frequency range than dichloromethane. The baseline-corrected integrated absorption coefficients measured for the corresponding 990–1130 cm^{-1} band segments of the two solution spectra are in excellent agreement.

(99+%), α -pinene (99+%), methacrolein (95%), and triethyl phosphate (99+%), Aldrich Chemical Co.; 1,3,5-trimethylbenzene, Eastman; diethyl phosphate (98.3%), Chem Service; and NO ($\geq 99.0\%$), propene ($\geq 99.0\%$), and 1-butene ($\geq 99.0\%$), Matheson Gas Products. Methyl nitrite, 2-propyl nitrite, and N_2O_5 were prepared and stored as described previously,^{8,10,13,14} and O_3 in O_2 diluent was generated using a Welsbach T-408 ozone generator. NO_2 was prepared as needed by reacting NO with an excess of O_2 .

Results

Photolysis and Dark Reactions. No decays ($< 5\%$) of gas-phase DEMP, DEEP, or TEP were observed in a ~ 7000 L Teflon chamber in either the dark over a period of 5.6 h or during 60 min of photolysis using the same light intensity and spectral distribution as used in the OH radical rate constant determinations in the same chamber. (The total durations of the photolysis experiments were 3.5–3.6 h.) These results show that dark losses of DEMP, DEEP, and TEP to the walls of the Teflon chamber were of negligible importance during all experiments and that any photolysis of DEMP, DEEP, and TEP over the ≤ 13 min irradiations of CH_3ONO - NO -organophosphorus compound-reference compound-air mixtures was also negligible.

Rate Constants for the Reactions of OH Radicals with DEMP, DEEP, and TEP. A series of CH_3ONO - NO -organophosphorus compound-reference compound-air irradiations were carried out in the ~ 7000 L Teflon chamber, with α -pinene and 1,3,5-trimethylbenzene as the reference compounds, and the data obtained are plotted in accordance with eq 1 in Figures 2 and 3. No effects of O_2 content (6–78%) or of relative humidity (5–50%) on the rate constant ratios were observed. α -Pinene and 1,3,5-trimethylbenzene, and α -pinene and di-*n*-butyl ether (the latter to serve as an additional check on the system), were present together as reference compounds

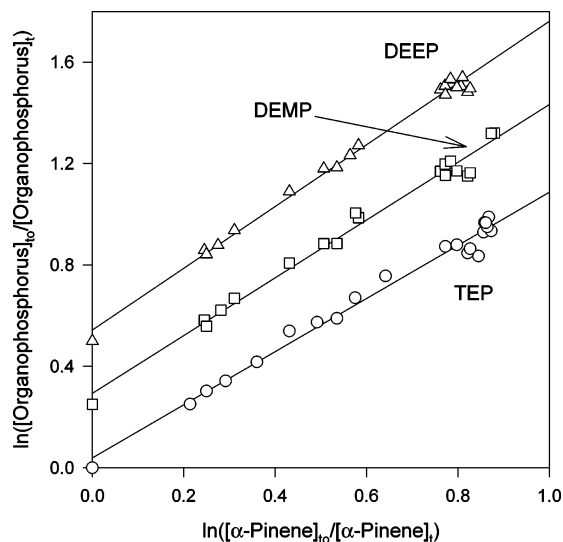


Figure 2. Plots of eq I for the reactions of OH radicals with diethyl methylphosphonate (DEMP), diethyl ethylphosphonate (DEEP), and triethyl phosphate (TEP), with α -pinene as the reference compound. The data for DEMP and DEEP have been displaced vertically by 0.25 and 0.50 units, respectively, for clarity.

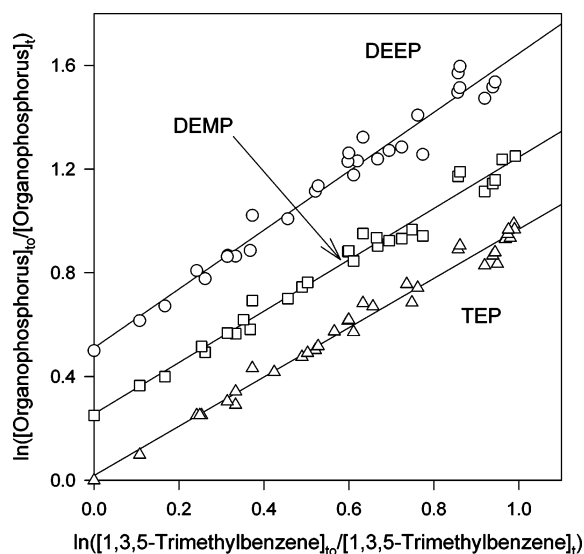


Figure 3. Plots of eq I for the reactions of OH radicals with diethyl methylphosphonate (DEMP), diethyl ethylphosphonate (DEEP), and triethyl phosphate (TEP), with 1,3,5-trimethylbenzene as the reference compound. The data for DEMP and DEEP have been displaced vertically by 0.25 and 0.50 units, respectively, for clarity.

in three experiments each, and hence rate constants for the reactions of OH radicals with 1,3,5-trimethylbenzene and di-*n*-butyl ether could be obtained relative to that for α -pinene (Figure 4). Similarly, in a number of experiments two or three of the organophosphorus compounds were present in the reactant mixtures, and hence rate constant ratios for the reactions of DEEP and TEP relative to DEMP and for the reaction of TEP relative to DEEP could be obtained (see, for example, the data plotted in Figure 5). Least-squares analyses of the experimental data lead to the rate constant ratios k_1/k_2 given in Table 1. These rate constant ratios k_1/k_2 are placed on an absolute basis by use of rate constants k_2 for the reactions of OH radicals with α -pinene and 1,3,5-trimethylbenzene at 296 K of $5.28 \times 10^{-11} \text{ cm}^3 \text{ molecule}^{-1} \text{ s}^{-1}$ and $5.67 \times 10^{-11} \text{ cm}^3 \text{ molecule}^{-1} \text{ s}^{-1}$, respectively.¹ The resulting rate constants k_1 are given in Table

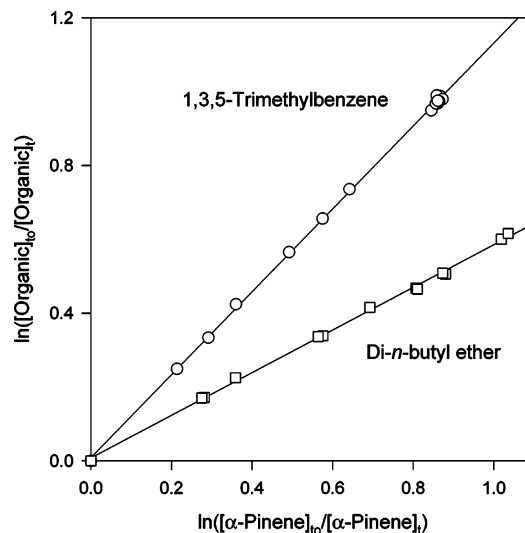


Figure 4. Plots of eq I for the reactions of OH radicals with 1,3,5-trimethylbenzene and di-*n*-butyl ether, with α -pinene as the reference compound.

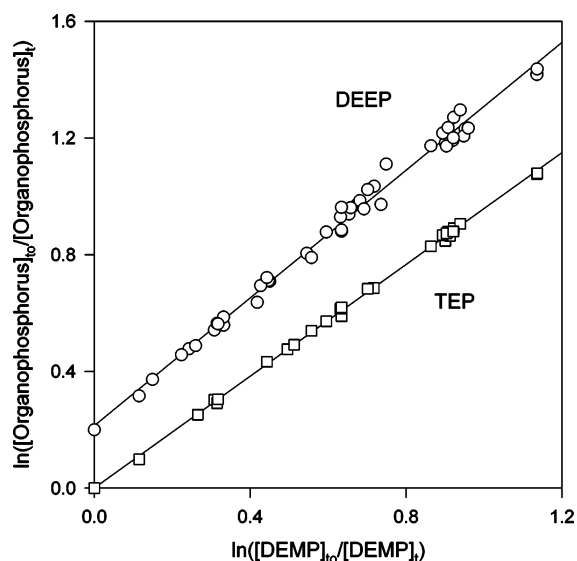


Figure 5. Plots of eq I for the reactions of OH radicals with diethyl ethylphosphonate (DEEP) and triethyl phosphate (TEP), with diethyl methylphosphonate (DEMP) as the reference compound. The data for DEEP have been displaced vertically by 0.20 units for clarity.

1, and it can be seen that the rate constants obtained with 1,3,5-trimethylbenzene and α -pinene as the reference compounds are in excellent agreement.

Rate Constant for the Reactions of NO₃ Radicals with DEMP, DEEP and TEP. Reactions of N₂O₅–NO₃–NO₂–organophosphorus compound–methacrolein–air mixtures and of an N₂O₅–NO₃–NO₂–TEP–propene–1-butene–air mixture were carried out in the same Teflon chamber as used for the OH radical rate constant determinations. The percentage losses of the organophosphorus compound were significantly less than those of the reference compounds (with maximum reactive losses of DEMP, DEEP, and TEP of 21% compared to up to 86% for methacrolein and a maximum reactive loss of TEP of 8% compared to up to 88% and 94% for propene and 1-butene, respectively). Least-squares analyses of these data lead to the rate constant ratios k_1/k_2 given in Table 2. These rate constant ratios are placed on an absolute basis by use of rate constants at 296 K for the NO₃ radical reactions of methacrolein, $3.4 \times$

TABLE 1: Rate Constant Ratios k_1/k_2 and Rate Constants k_1 for the Reactions of OH Radicals with DEMP, DEEP, and Triethyl Phosphate at 296 ± 2 K

| organophosphorus compound | reference compound | k_1/k_2^a | $10^{11}k_1$ (cm ³ molecule ⁻¹ s ⁻¹) |
|----------------------------------|------------------------|-------------------|--|
| diethyl methylphosphonate (DEMP) | α -pinene | 1.14 ± 0.07 | 6.02 ± 0.37 |
| | 1,3,5-trimethylbenzene | 0.990 ± 0.053 | 5.61 ± 0.31 |
| diethyl ethylphosphonate (DEEP) | α -pinene | 1.22 ± 0.06 | 6.44 ± 0.32 |
| | 1,3,5-trimethylbenzene | 1.14 ± 0.08 | 6.46 ± 0.46 |
| triethyl phosphate (TEP) | α -pinene | 1.05 ± 0.06 | 5.54 ± 0.32 |
| | 1,3,5-trimethylbenzene | 0.951 ± 0.042 | 5.39 ± 0.24 |
| 1,3,5-trimethylbenzene | α -pinene | 1.12 ± 0.02 | 5.91 ± 0.11 |
| di- <i>n</i> -butyl ether | α -pinene | 0.578 ± 0.014 | 3.05 ± 0.08 |
| DEEP | DEMP | 1.09 ± 0.04 | |
| TEP | DEMP | 0.958 ± 0.012 | |
| TEP | DEEP | 0.866 ± 0.026 | |

^a Indicated errors are two least-squares standard deviations. ^b Placed on an absolute basis by use of rate constants at 296 K of $k_2(\alpha\text{-pinene}) = 5.28 \times 10^{-11}$ cm³ molecule⁻¹ s⁻¹ and $k_2(1,3,5\text{-trimethylbenzene}) = 5.67 \times 10^{-11}$ cm³ molecule⁻¹ s⁻¹.

TABLE 2: Rate Constant Ratios k_1/k_2 and Rate Constants k_1 for the Reactions of NO₃ Radicals with DEMP, DEEP, and TEP at 296 ± 2 K

| organophosphorus compound | reference compound | k_1/k_2^a | $10^{16}k_1$ (cm ³ molecule ⁻¹ s ⁻¹) |
|----------------------------------|-----------------------|-------------------|--|
| diethyl methylphosphonate (DEMP) | methacrolein | 0.11 ± 0.03 | 3.7 ± 1.1 |
| diethyl ethylphosphonate (DEEP) | methacrolein | 0.10 ± 0.04 | 3.4 ± 1.4 |
| triethyl phosphate (TEP) | methacrolein | 0.07 ± 0.04 | 2.4 ± 1.4 |
| | propene ^c | 0.038 ± 0.009 | 3.5 ± 0.9^c |
| | 1-butene ^c | 0.029 ± 0.007 | 3.8 ± 1.0^c |

^a Indicated errors are two least-squares standard deviations. ^b Placed on an absolute basis by use of rate constants at 296 K of $k_2(\text{methacrolein}) = 3.4 \times 10^{-15}$ cm³ molecule⁻¹ s⁻¹,^{1,15} $k_2(\text{propene}) = 9.24 \times 10^{-15}$ cm³ molecule⁻¹ s⁻¹,¹ and $k_2(1\text{-butene}) = 1.32 \times 10^{-14}$ cm³ molecule⁻¹ s⁻¹.¹ ^c From a single experiment with propene and 1-butene as reference compounds.

10^{-15} cm³ molecule⁻¹ s⁻¹,^{1,15} propene, 9.24×10^{-15} cm³ molecule⁻¹ s⁻¹,¹ and 1-butene, 1.32×10^{-14} cm³ molecule⁻¹ s⁻¹.¹ The resulting rate constants k_1 are also given in Table 2.

Rate Constants for Reactions of O₃ with DEMP, DEEP, and TEP. No decays (<5%) of gas-phase DEMP, DEEP, or TEP were measured in the ~ 7000 L Teflon chamber in the presence of $(4.64\text{--}5.17) \times 10^{13}$ molecules cm⁻³ of O₃ over 297–305 min reaction periods. Use of an upper limit of 5% for the amount of DEMP, DEEP, or TEP reacted over these time periods results in upper limits to the rate constants for reaction of O₃ with DEMP, DEEP, and TEP of $k_3 < 6 \times 10^{-20}$ cm³ molecule⁻¹ s⁻¹ at 296 ± 2 K.

Products of the Reaction of OH Radicals with DEMP, DEEP, and TEP. API-MS Analyses. Irradiations of CH₃ONO–NO–DEMP, DEEP, or TEP–air mixtures were carried out in a second ~ 7000 L Teflon chamber at $\sim 5\%$ relative humidity with analyses by in situ API-MS. In the positive ion mode, API-MS spectra of these mixtures prior to irradiation showed the protonated organophosphorus compound dimer at 305 u (DEMP), 333 u (DEEP), and 365 u (TEP), with no additional ion peaks being observed after irradiation due to reaction products.

In the negative ion mode, no ion peaks attributed to DEMP, DEEP, or TEP were observed prior to irradiation. Negative ion API-MS spectra of irradiated CH₃ONO–NO–air mixtures of DEMP, DEEP, and TEP after 1 min irradiation are shown in Figure 6. Addition of 1.7×10^{13} molecules cm⁻³ of NO₂ to the chamber changed the relative intensity of certain of these ion peaks (for example, those at 280 and 294 u in the DEMP reaction, at 308 and 322 u in the DEEP reaction, and at 340 and 354 u in the TEP reaction) because of differing relative concentrations of O₂⁻, NO₂⁻, and NO₃⁻ reagent ions. API-MS/MS “product ion” and “precursor ion” spectra of the ion peaks shown in Figure 6 were obtained and, as an example, API-MS/MS “product ion” spectra of the 294, 322, and 354 u ion peaks observed in the API-MS spectra of the DEMP, DEEP, and TEP reactions, respectively, are shown in Figure 7. For the DEMP,

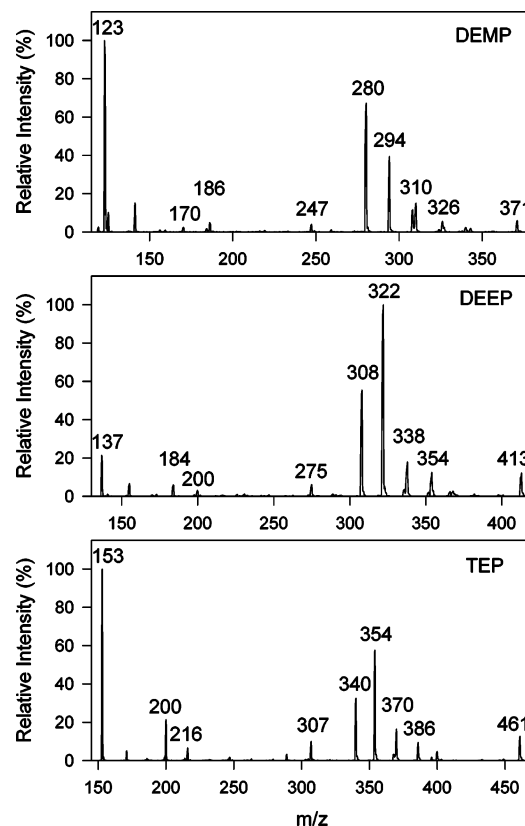


Figure 6. Negative ion API-MS spectra of irradiated CH₃ONO–NO–diethyl methylphosphonate–air, CH₃ONO–NO–diethyl ethylphosphonate–air and CH₃ONO–NO–triethyl phosphate–air mixtures after 1 min of irradiation (see text for ion peak assignments).

DEEP, and TEP reactions, all of the ion peaks due to reaction product(s) in the API-MS spectra shown in Figure 6 can be attributed as arising from a single product from each reaction, of molecular weight 124 (DEMP reaction), 138 (DEEP reaction),

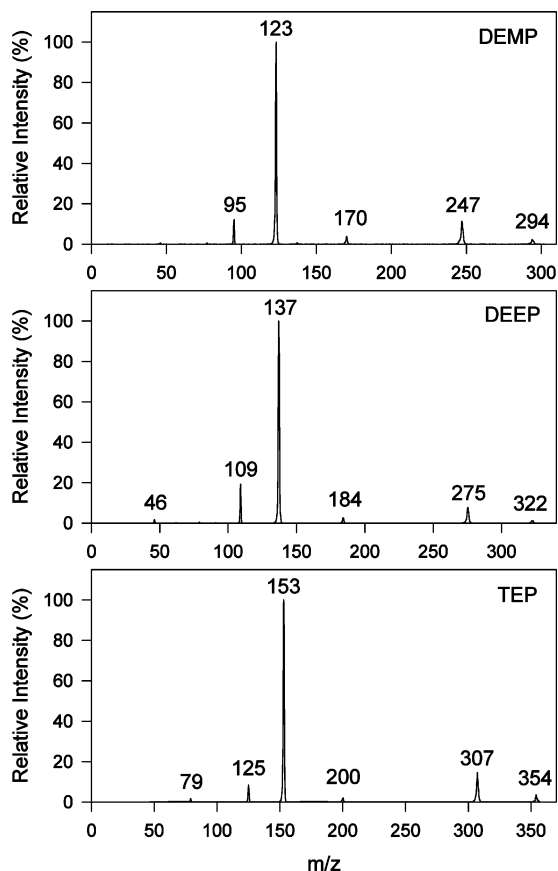


Figure 7. Negative ion API-MS/MS "product ion" spectra of the 294 u (diethyl methylphosphonate), 322 u (diethyl ethylphosphonate), and 354 u (triethyl phosphate) ion peaks present in the API-MS spectra shown in Figure 6.

and 154 (TEP reaction), and these are attributed to $C_2H_5OP(O)(CH_3)OH$ (ethyl methylphosphonate) from the DEMP reaction, $C_2H_5OP(O)(C_2H_5)OH$ (ethyl ethylphosphonate) from the DEEP reaction, and $(C_2H_5O)_2P(O)OH$ (diethyl phosphate, DEP) from the TEP reaction. As an example, the assignments of the ion peaks shown in Figure 6 for the TEP reaction are 153 u, $[154 - H]^-$ (i.e., $(C_2H_5O)_2P(O)O^-$); 200 u, $[154 + NO_2]^-$; 216 u, $[154 + NO_3]^-$; 307 u, $[154 + 154 - H]^-$; 340 u, $[154 + 154 + O_2]^-$; 354 u, $[154 + 154 + NO_2]^-$; 370 u, $[154 + 154 + NO_3]^-$; 386 u, $[154 + 154 + NO_2 + O_2]^-$; and 461 u, $[154 + 154 + 154 - H]^-$, with analogous assignments for the ion peaks in the DEMP and DEEP reactions.

An API-MS spectrum of diethyl phosphate (DEP) introduced into the chamber in the presence of NO_x is shown in Figure 8 together with the API-MS spectrum of an irradiated $CH_3ONO-NO-TEP$ -air mixture. Identical ion peaks are present in both spectra, and API-MS/MS product ion spectra of the ion peaks observed in the API-MS spectra are also identical, as shown for the 354 u ion peaks in Figure 9. These data confirm that DEP $[(C_2H_5O)_2P(O)OH]$ is the product observed from the OH radical-initiated reaction of TEP, and by analogy the products of the DEMP and DEEP reactions are $C_2H_5OP(O)(CH_3)OH$ and $C_2H_5OP(O)(C_2H_5)OH$, respectively.

FT-IR and GC-FID Analyses of the Reaction of OH Radicals with TEP. These experiments were carried out in a 5870 L Teflon-coated evacuable chamber. The quantitative analysis of products and reactants by FT-IR spectroscopy was carried out by a subtractive procedure. Components were successively subtracted from the spectrum of the mixture using calibrated spectra of the gaseous reactants and known products,

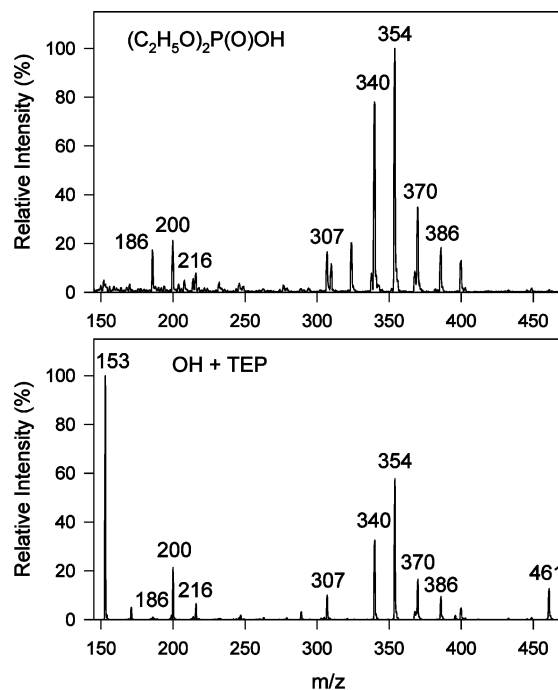


Figure 8. Negative ion API-MS spectra of diethyl phosphate (DEP) introduced into the chamber in the presence of NO_x and of an irradiated $CH_3ONO-NO$ -triethyl phosphate-air mixture after 1 min of irradiation.

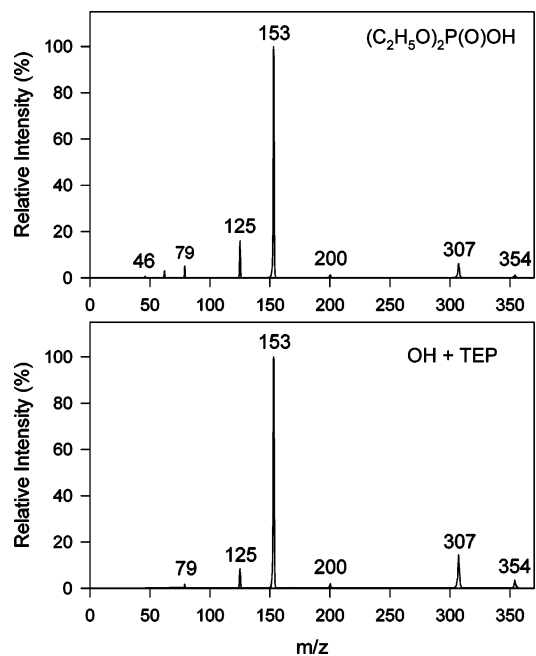


Figure 9. Negative ion API-MS/MS "product ion" spectrum of the 354 u ion peaks present in the API-MS spectra shown in Figure 8.

which have been recorded previously with the same instrument and identical spectral parameters. As routinely carried out, the absorption bands of CH_3ONO and NO and of their irradiation products NO_2 , $HCHO$, CH_3ONO_2 , HNO_3 , and $HONO$ were subtracted first to reveal more clearly the products from the main reactant. Readily identified products were CO_2 (a major product), CO , and $CH_3C(O)OONO_2$ (PAN, peroxyacetyl nitrate). Characteristic group frequencies also suggested the formation of organic nitrates, $RONO_2$, at 1680, 1295, and 827 cm^{-1} and an organic ester, most likely $ROC(O)CH_3$, at 1795 and 1210 cm^{-1} as minor products. $HCHO$ was also determined by FT-IR

spectroscopy as a major product in irradiations employing $(\text{CH}_3)_2\text{CHONO}$ instead of CH_3ONO as the OH radical precursor.

CH_3CHO , a minor product, has a weak infrared absorption and was measured by GC-FID. Experiments carried out in a ~ 7000 L Teflon chamber with GC-FID analyses showed that the formation yield of CH_3CHO in air (21% O_2 content) at $\sim 5\%$ relative humidity and in synthetic air with 6% O_2 content (at $\leq 2\%$ relative humidity) was $11 \pm 2\%$, where the indicated errors are two least-squares standard deviations combined with estimated uncertainties in the GC-FID response factors for TEP and CH_3CHO of $\pm 5\%$ each, and the measured CH_3CHO concentrations have been corrected for secondary reaction with OH radicals (the maximum correction being 18%).

Subtraction of the spectrum of the unreacted TEP revealed $(\text{C}_2\text{H}_5\text{O})_2\text{P}(\text{O})\text{OH}$ (DEP) as a product by comparison with the IR spectrum of DEP introduced into the chamber. The analyses of TEP and its major product DEP were not straightforward. Their major infrared absorption bands, found in the $900\text{--}1100$ cm^{-1} region, severely overlap, and both compounds exhibited significant decay to the wall of the evacuable chamber. Because of its significant decay in this evacuable chamber, the FT-IR calibrations for TEP were referenced to the GC-FID analyses of samples taken contemporaneously with the spectra recorded. GC-FID calibrations of TEP were performed independently and more accurately in a 7000 L Teflon chamber where TEP decay was minimal (see above). It should be noted that the inside surface of the evacuable chamber consists of Teflon-coated aluminum together with quartz windows and gold-coated mirror surfaces of the multiple reflection optical system and with a number of "O"-ring seals for various flanges (including the end-window assemblies). It is possible that the dark decays of the organophosphorus compounds studied here involved absorption into these "O"-rings.

Since wall losses of TEP occurred during the dark periods when GC-FID analyses were conducted (~ 40 min on average), corrections to the actual amount of TEP consumed during each irradiation period were obtained from the decay rate of TEP which was established for each experiment by relative IR intensity measurements prior to the irradiation. The measured initial decay rates of TEP after injection into the evacuable chamber depended unpredictably on wall conditioning, with initial rates of $(1\text{--}1.3) \times 10^{-3}$ min^{-1} being observed for the chamber injected with TEP after numerous other types of experiments have been carried out and for TEP runs with diluent air at 5% relative humidity. However, for the majority of the experiments where TEP remained in the chamber for ~ 1 h or more prior to irradiation, a slower decay rate in the range $(4\text{--}6) \times 10^{-4}$ min^{-1} was established. Calculations using these later decay rates for the individual runs resulted in 8–14% corrections to the amounts of TEP consumed by the reaction as obtained from the GC-FID analyses alone.

Using these procedures, the products observed and their yields were DEP, 65–82% (initial, see below); CO_2 , $80 \pm 10\%$; HCHO, $55 \pm 5\%$; CH_3CHO , $11 \pm 3\%$ (by GC-FID analyses from the evacuable chamber experiments, in excellent agreement with the $11 \pm 2\%$ yield obtained in the Teflon chamber, see above); CO, $11 \pm 3\%$; PAN, 8%; RONO_2 , 7%; and $\text{ROC}(\text{O})\text{CH}_3$, 4%.

The formation of several products from a $\text{CH}_3\text{ONO}\text{--NO}\text{--TEP}\text{--air}$ irradiation is shown in Figure 10. Traces A and B of Figure 10 are reference spectra of TEP and DEP, respectively. Figure 10C is the product spectrum after 1.2×10^{13} molecules cm^{-3} of TEP had reacted. The absorption bands of the unreacted

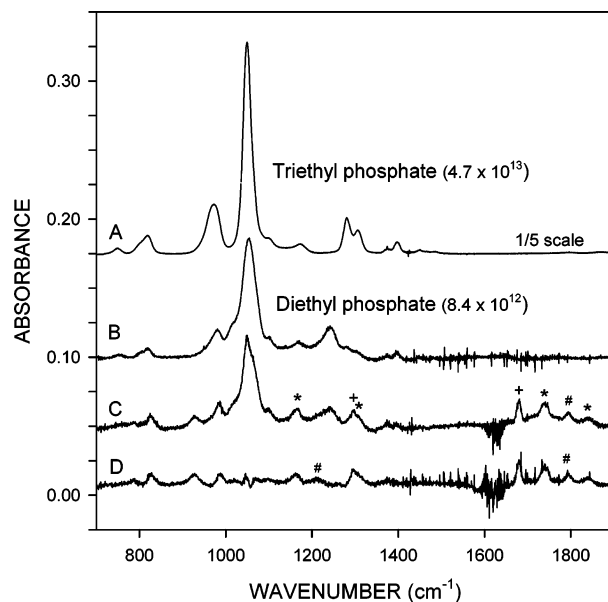


Figure 10. (A) Triethyl phosphate (TEP) reference spectrum. (B) Diethyl phosphate (DEP) reference spectrum. Numbers in parentheses are concentrations in molecules cm^{-3} . (C) Product spectrum from an irradiated $\text{CH}_3\text{ONO}\text{--NO}\text{--TEP}\text{--air}$ mixture, with 1.2×10^{13} molecules cm^{-3} of TEP consumed and 5.4×10^{12} molecules cm^{-3} of DEP present. Symbols indicate the characteristic band positions of the minor products PAN (*), RONO_2 (+), and $\text{ROC}(\text{O})\text{CH}_3$ (#). (D) From (C) after subtraction of the DEP absorption band. See text for details.

starting compounds, HCHO, and other products from CH_3ONO and NO (see above) have been subtracted in Figure 10C, together with the weak CH_3CHO absorptions per the GC-FID analyses. Thus, the presence of 5.4×10^{12} molecules cm^{-3} of DEP is shown in Figure 10C, with the weaker but distinct signals from the minor products PAN, RONO_2 , and $\text{RC}(\text{O})\text{OCH}_3$ also identified in this spectrum and in Figure 10D where the absorption bands of DEP have been subtracted. The absorption bands of CO_2 , a major product, are outside the range of the plots. The measured concentrations of HCHO and CH_3CHO were corrected for secondary reaction with the OH radical (with maximum corrections of 7% and 8%, respectively) using OH radical reaction rate constants for HCHO and CH_3CHO (cm^3 molecule $^{-1}$ s $^{-1}$) of 8.5×10^{-12} and 1.5×10^{-11} , respectively.¹⁵ The cited uncertainties are two least-squares standard deviations combined with estimated uncertainties in the TEP, CO_2 , HCHO, CH_3CHO , and CO concentrations of TEP, $\pm 5\%$; CO_2 , $\pm 7\%$ (which includes calibration errors and errors due the nonlinearity inherent to the finely structured CO_2 band at 2350 cm^{-1}); HCHO, $\pm 5\%$; CH_3CHO , $\pm 5\%$; and CO, $\pm 7\%$ (including the calibration error and nonlinearity inherent to its highly resolved band at 2145 cm^{-1}). The effect of ambient CO_2 on the product CO_2 measurements was minimized by stabilizing the N_2 purge of the FT-IR instrument for a period of at least 90 min prior to the measurements. CO_2 contributions from the photolysis of CH_3ONO and $(\text{CH}_3)_2\text{CHONO}$ were negligible, as determined from the CO_2 yields from separate photolyses of $\text{CH}_3\text{ONO}\text{--NO}\text{--air}$ and $(\text{CH}_3)_2\text{CHONO}\text{--NO}\text{--air}$ mixtures.

These product yields were derived from four irradiation experiments carried out with dry diluent air. A number of experiments were carried out in diluent air at 5% relative humidity to see whether the presence of water vapor leads to $\text{HC}(\text{O})\text{OH}$ as a secondary product. $\text{HC}(\text{O})\text{OH}$ was not positively detected in either dry or humidified diluent air, and its upper limit yield was estimated to be $< 2\%$ in both dry air and in air at 5% relative humidity. The 65% and 82% yields of DEP given

TABLE 3: Room Temperature Rate Constants k_1 for the Reactions of OH Radicals with DEMP, DEEP, and TEP, Compared with Literature Values

| organophosphorus compound | $10^{11}k_1$ (cm ³ molecule ⁻¹ s ⁻¹) | | reference |
|----------------------------------|--|--------------------------|------------------------------------|
| | this work ^a | literature | |
| diethyl methylphosphonate (DEMP) | 5.78 ± 0.24 | 3.23 ± 0.11 ^b | Kleindienst and Smith ⁷ |
| diethyl ethylphosphonate (DEEP) | 6.45 ± 0.27 | | |
| triethyl phosphate (TEP) | 5.44 ± 0.20 | 5.53 ± 0.35 ^c | Atkinson et al. ⁶ |

^a Weighted averages of the two rate constants measured relative to those for 1,3,5-trimethylbenzene and α -pinene (Table 1). ^b At \sim 298 K. Relative to the rate constants for reactions of OH radicals with *n*-hexane, propene, and 1,3-butadiene. The rate constant used for the reaction of OH radicals with *n*-hexane was 3% higher than a more recent recommendation.¹ ^c At 296 ± 2 K. Relative to the reaction of OH radicals with propene, using a rate constant of $k_2(\text{propene}) = 2.66 \times 10^{-11}$ cm³ molecule⁻¹ s⁻¹.

above are results from the first irradiation periods of two separate experiments. These two values are in agreement within the overall uncertainties of the measurements, i.e., the estimated 20% calibration error for DEP, the 5% uncertainty associated with each FT-IR measurement of TEP as referenced to the nominal \pm 5% error of the GC-FID analysis of TEP, and the additional error associated with the correction for TEP decay in the evacuable chamber which occurred between the GC-FID measurements. More importantly, a large uncertainty would arise from the decay of DEP to the chamber walls which occurred while it was being formed and monitored, as evidenced by the drastically lower yields of DEP which were measured during the subsequent irradiation periods for both experiments (with measured yields of 82 and 44% in one experiment and 65%, 49%, and 30% in the second experiment). While DEP is also expected to react with OH radicals, no data are available for the kinetics of this reaction, and hence no corrections for secondary reaction of DEP with OH radicals were made. However, the observed decreases in DEP formation yield with increasing extent of reaction were almost certainly largely due to wall losses and not secondary reactions.

The quantitative estimate of the yield of organic nitrates (RONO₂) was made by measuring the area of the 1680 cm⁻¹ band and applying the average integrated absorption coefficient of 2.5×10^{-17} cm molecule⁻¹, derived from the corresponding absorption bands of a series of organic nitrates.¹⁶ Likewise, the quantitative estimate of the formation yield of acetate (ROC(O)-CH₃) species was obtained from the 1795 cm⁻¹ band using the integrated absorption coefficient of 2.3×10^{-17} cm molecule⁻¹, an average derived from the corresponding absorption band areas of ethyl acetate, allyl acetate, and 3-chloropropyl acetate (with the individual absorption coefficients agreeing within 10% of each other).

Discussion

Our rate constant ratio of $k(\text{OH} + 1,3,5\text{-trimethylbenzene})/k(\text{OH} + \alpha\text{-pinene}) = 1.12 \pm 0.02$ is in excellent agreement with the value of 1.07 derived from the literature OH radical reaction rate constants.¹ Furthermore, the rate constant obtained here for the reaction of OH radicals with di-*n*-butyl ether of 3.05×10^{-11} cm³ molecule⁻¹ s⁻¹ is in excellent agreement with the literature room temperature rate constants of (in units of 10^{-11} cm³ molecule⁻¹ s⁻¹) 2.78 ± 0.36,¹⁷ 2.68 ± 0.32,¹⁸ 2.72 ± 0.02,¹⁹ 2.68 ± 0.12,¹⁹ 3.22 ± 0.10,²⁰ 2.91 ± 0.15,²⁰ 2.69 ± 0.22,²¹ and 3.26 ± 0.25²² (where relative rate measurements have been reevaluated using the most recent recommendations for the reference compounds used).

The rate constants measured here for the reactions of NO₃ radicals and O₃ with DEMP, DEEP, and TEP and for the reaction of OH radicals with DEEP are the first reported. The observed lack of reaction with O₃ is consistent with previous data for the reactions of O₃ with (CH₃O)₃PO, (CH₃O)₃PS,

(CH₃O)₂P(O)SCH₃, (CH₃S)₂P(O)OCH₃, and (CH₃O)₂P(S)-SCH₃.^{4,5} This study is the first to observe a reaction of NO₃ radicals with an alkyl phosphate, alkyl phosphorothioate, or alkyl phosphonate, with previous studies of the reactions of NO₃ radicals with (CH₃O)₃PS, (CH₃O)₂P(O)SCH₃, (CH₃S)₂P(O)-OCH₃, and (CH₃O)₂P(S)SCH₃ having obtained only upper limits to the rate constants, of $<(1-30) \times 10^{-15}$ cm³ molecule⁻¹ s⁻¹,⁵ factors of 2.5–77 higher than the actual rate constants measured here for DEMP, DEEP, and TEP.

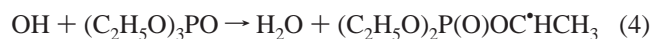
The rate constants measured here for the reactions of OH radicals with DEMP, DEEP, and TEP are given in Table 3 (these being weighted averages of the two individual measurements with 1,3,5-trimethylbenzene and α -pinene as reference compounds), and those for DEMP and TEP are compared with the available literature values.^{6,7} Our present rate constant for TEP is in excellent agreement with our previous measurement⁶ determined relative to the rate constant for the reaction of OH radicals with propene. Furthermore, combining the present rate constant ratio of $k_1(\text{TEP})/k_2(1,3,5\text{-trimethylbenzene}) = 0.951 \pm 0.042$ with the rate constant ratio $k_2(1,3,5\text{-trimethylbenzene})/k_2(\text{propene}) = 2.16 \pm 0.11$ at 296 ± 2 K²³ results in $k_1(\text{TEP})/k_2(\text{propene}) = 2.05 \pm 0.14$, in excellent agreement with our previous value of this rate constant ratio of 2.08 ± 0.13 .⁶ However, for the reaction of OH radicals with DEMP our room temperature rate constant of 5.78×10^{-11} cm³ molecule⁻¹ s⁻¹ is a factor of 1.8 higher than that reported by Kleindienst and Smith,⁷ for reasons that are presently not known.

There is a large increase in the room temperature OH radical reaction rate constant when the methyl groups in trimethyl phosphate (7.4×10^{-12} cm³ molecule⁻¹ s⁻¹)⁴ are replaced by ethyl groups in triethyl phosphate (5.5×10^{-11} cm³ molecule⁻¹ s⁻¹ [Table 3]). However, as evident from Table 1, there is only a 9 ± 4% increase in replacing the methyl group bonded directly to the P atom in DEMP by the ethyl group in DEEP, and DEEP is actually more reactive than TEP (by 15 ± 4%). It therefore appears that the reaction of OH radicals with DEMP, DEEP, and triethyl phosphate proceed mainly by H atom abstraction from the CH₂ portion of the CH₃CH₂O– groups. Using the approach of Kwok and Atkinson²⁴ and assuming that the partial OH radical rate constants for the two CH₃CH₂O– groups in DEEP and DEMP are identical, then the 9 ± 4% increase in rate constant from DEMP to DEEP suggests that \sim 9% of the overall OH radical reaction with DEEP proceeds by H atom abstraction from the C₂H₅ group attached directly to the P atom. The room temperature OH radical reaction partial rate constants per CH₃CH₂O– group are then 2.9×10^{-11} cm³ molecule⁻¹ s⁻¹ for DEEP and DEMP and 1.8×10^{-11} cm³ molecule⁻¹ s⁻¹ for TEP.

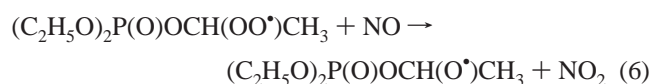
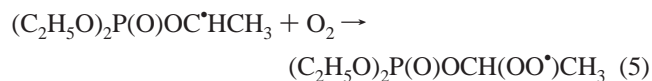
Our product study of the reactions of OH radicals with DEMP, DEEP, and TEP in air at \sim 5% relative humidity using in situ API-MS observed product ion peaks attributed to ethyl methylphosphonate [C₂H₅OP(O)(CH₃)OH] from DEMP, ethyl

ethylphosphonate [$C_2H_5OP(O)(C_2H_5)OH$] from DEEP, and diethyl phosphate [DEP, $(C_2H_5O)_2P(O)OH$] from TEP, with the formation of DEP from TEP being confirmed by matching the API-MS and API-MS/MS spectra and FT-IR spectra of the reaction products with those of an authentic standard. The products observed and quantified from the reaction of OH radicals with TEP using in situ FT-IR analyses and GC-FID analyses account for $\sim 82 \pm 15\%$ of the product carbon and 65–82% of the product phosphorus at the first analysis time and a higher percentage if significant losses of DEP occurred prior to the first analysis period in each of the experiments.

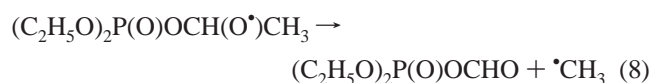
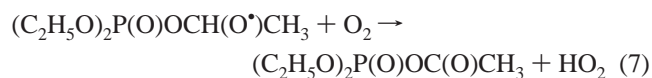
Our kinetic and product data are consistent with the OH radical reactions with DEMP, DEEP, and TEP proceeding mainly by H atom abstraction from the C–H bonds of the CH_2 groups in the C_2H_5O moieties. Using TEP as the example



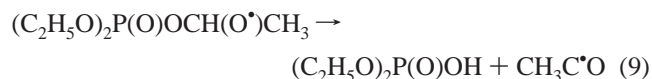
followed by addition of O_2 and reaction with NO to form (mainly) the alkoxy radical



This alkoxy radical could react with O_2 or decompose



with $(C_2H_5O)_2P(O)OC(O)CH_3$ and $(C_2H_5O)_2P(O)OCHO$ reacting with water vapor to form DEP and acetic acid or DEP and formic acid, respectively. The methyl radical formed from the alkoxy radical decomposition reaction will form HCHO (plus some methyl nitrite and methyl nitrate from reactions of the CH_3O^* radical with NO and NO_2). The lack of formation of formic acid rules out the decomposition reaction followed by hydrolysis of $(C_2H_5O)_2P(O)OCHO$, and the formation of significant yields of HCHO indicates that the alkoxy radical reaction with O_2 (reaction 7) is also not dominant. An additional reaction of the alkoxy radical is via the rearrangement analogous to that observed for the alkoxy radicals of structure $RC(O)-OCH(O^*)R'$ formed from esters,^{25,26} to form DEP + CH_3C^*O .

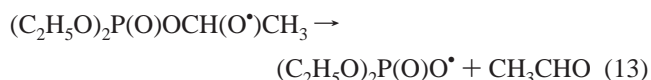


In the presence of NO and NO_2 the acetyl radical leads to PAN ($CH_3C(O)OONO_2$) or HCHO + CO_2 (depending on the NO/ NO_2 ratio)¹⁵



with subsequent reactions of the methyl radical leading to the formation of HCHO plus (depending on the NO and NO_2 concentrations) methyl nitrite and methyl nitrate (from reactions of the CH_3O^* radical with NO and NO_2 , respectively, competing with the reaction with O_2 to form HCHO).¹⁵

Our product data, namely the high yields of DEP (65–82% initial), CO_2 ($80 \pm 10\%$), and HCHO ($55 \pm 5\%$) and the observation of PAN in 8% yield, suggest that reaction 9 accounts for ~ 80 –90% of the overall reaction, leading to DEP plus either PAN or $CO_2 + HCHO$ (and methyl nitrite and methyl nitrate). The formation of acetaldehyde, in $11 \pm 2\%$ yield, must arise from another reaction pathway, possibly decomposition of the $(C_2H_5O)_2P(O)OCH(O^*)CH_3$ radical (note that the low yield of acetaldehyde also means that a direct addition–elimination pathway is not significant).



While reactions analogous to reaction 9 appear to occur in the OH radical-initiated reactions of DEMP and DEEP (as evidenced by our API-MS analyses), a reaction analogous to reaction 9 may not occur for $\text{P}(O)OCH_2O^*$ alkoxy radicals; rather, these radicals may form $\text{P}(O)OCHO$ which then hydrolyzes to form $\text{P}(O)OH + HC(O)OH$.

Acknowledgment. This work was supported by ENSCO, Inc., with preliminary work being funded by the California Air Resources Board through Contract No. 99-330 (initial API-MS product study of TEP) and by Science Applications International Corp. While this research has been funded by these agencies, the results and content of this publication do not necessarily reflect the views and opinions of the funding agencies. R.A. thanks the University of California Agricultural Experiment Station for partial salary support.

References and Notes

- (1) Atkinson, R.; Arey, J. *Chem. Rev.* **2003**, *103*, 4605.
- (2) Toy, A. D.; Walsh, E. N. *Phosphorus Compounds in Everyday Living*; American Chemical Society: Washington, DC, 1987.
- (3) *The Pesticide Manual*, 9th ed.; Worthing, C. R., Hance, R. J., Eds.; British Crop Protection Council, 1991.
- (4) Tuazon, E. C.; Atkinson, R.; Aschmann, S. M.; Arey, J.; Winer, A. M.; Pitts, J. N., Jr. *Environ. Sci. Technol.* **1986**, *20*, 1043.
- (5) Goodman, M. A.; Aschmann, S. M.; Atkinson, R.; Winer, A. M. *Arch. Environ. Contam. Toxicol.* **1988**, *17*, 281.
- (6) Atkinson, R.; Aschmann, S. M.; Goodman, M. A.; Winer, A. M. *Int. J. Chem. Kinet.* **1988**, *20*, 273.
- (7) Kleindienst, T. E.; Smith, D. F. Chemical Degradation in the Atmosphere, Final Report on The Atmospheric Chemistry of Three Important Volatile Chemical Precursors to Applied Research Associates, Inc., U.S. Air Force Contract No. F08635-93-C-0020, Armstrong Laboratory Environics Directorate, Tyndall AFB, FL, Sept 1996.
- (8) Martin, P.; Tuazon, E. C.; Atkinson, R.; Maughan, A. D. *J. Phys. Chem. A* **2002**, *106*, 1542.
- (9) Aschmann, S. M.; Atkinson, R. *Int. J. Chem. Kinet.* **1998**, *30*, 533.
- (10) Atkinson, R.; Plum, C. N.; Carter, W. P. L.; Winer, A. M.; Pitts, J. N., Jr. *J. Phys. Chem.* **1984**, *88*, 1210.
- (11) Aschmann, S. M.; Chew, A. A.; Arey, J.; Atkinson, R. *J. Phys. Chem. A* **1997**, *101*, 8042.
- (12) Arey, J.; Aschmann, S. M.; Kwok, E. S. C.; Atkinson, R. *J. Phys. Chem. A* **2001**, *105*, 1020.
- (13) Aschmann, S. M.; Martin, P.; Tuazon, E. C.; Arey, J.; Atkinson, R. *Environ. Sci. Technol.* **2001**, *35*, 4080.
- (14) Taylor, W. D.; Allston, T. D.; Moscato, M. J.; Fazekas, G. B.; Kozlowski, R.; Takacs, G. A. *Int. J. Chem. Kinet.* **1980**, *12*, 231.
- (15) IUPAC, <http://www.iupac-kinetic.ch.cam.ac.uk/>.
- (16) Tuazon, E. C.; Atkinson, R. *Int. J. Chem. Kinet.* **1990**, *22*, 1221.

- (17) Wallington, T. J.; Liu, R.; Dagaut, P.; Kurylo, M. J. *Int. J. Chem. Kinet.* **1988**, *20*, 41.
- (18) Wallington, T. J.; Andino, J. M.; Skewes, L. M.; Siegl, W. O.; Japar, S. M. *Int. J. Chem. Kinet.* **1989**, *21*, 993.
- (19) Nelson, L.; Rattigan, O.; Neavyn, R.; Sidebottom, H.; Treacy, J.; Nielsen, O. J. *Int. J. Chem. Kinet.* **1990**, *22*, 1111.
- (20) Semadeni, M.; Stocker, D. W.; Kerr, J. A. *J. Atmos. Chem.* **1993**, *16*, 79.
- (21) Mellouki, A.; Teton, S.; Le Bras, G. *Int. J. Chem. Kinet.* **1995**, *27*, 791.
- (22) Harry, C.; Arey, J.; Atkinson, R. *Int. J. Chem. Kinet.* **1999**, *31*, 425.
- (23) Atkinson, R.; Aschmann, S. M. *Int. J. Chem. Kinet.* **1989**, *21*, 355.
- (24) Kwok, E. S. C.; Atkinson, R. *Atmos. Environ.* **1995**, *29*, 1685.
- (25) Tuazon, E. C.; Aschmann, S. M.; Atkinson, R.; Carter, W. P. L. *J. Phys. Chem. A* **1998**, *102*, 2316.
- (26) Christensen, L. K.; Ball, J. C.; Wallington, T. J. *J. Phys. Chem. A* **2000**, *104*, 345.